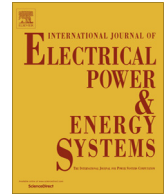




Contents lists available at ScienceDirect

Electrical Power and Energy Systems

journal homepage: www.elsevier.com/locate/ijepes

Power system voltage stability monitoring using artificial neural networks with a reduced set of inputs



A.R. Bahmanyar, A. Karami*

Faculty of Engineering, University of Guilan, P.O. Box: 41635-3756, Rasht, Iran

ARTICLE INFO

Article history:

Received 30 March 2013

Received in revised form 18 December 2013

Accepted 16 January 2014

Keywords:

Voltage stability

Artificial neural network

Saddle-node bifurcation

Feature selection

Gram–Schmidt orthogonalization process

Contingency analysis

ABSTRACT

This paper presents an artificial neural network (ANN)-based approach for online monitoring of a voltage stability margin (VSM) in electric power systems. The VSM is calculated by estimating the distance from the current operation state to the maximum voltage stability limit point according to the system loading parameter. Using the Gram–Schmidt orthogonalization process along with an ANN-based sensitivity technique, an efficient feature selection method is proposed to find the fewest input variables required to approximate the VSM with sufficient accuracy and high execution speed. Many algorithms have already been proposed in the literature for voltage stability assessment (VSA) using neural networks; however, the main drawback of the previously published works is that they need to train a new neural network when a change in the power system topology (configuration) occurs. Therefore, the possibility of employing a single ANN for estimating the VSM for several system configurations is investigated in this paper. The effectiveness of the proposed method is tested on the dynamic models of the New England 39-bus and the southern/eastern (SE) Australian power systems. The results obtained indicate that the proposed scheme provides a compact and efficient ANN model that can successfully and accurately estimate the VSM considering different system configurations as well as operating conditions, employing the fewest possible input features.

© 2014 Elsevier Ltd. All rights reserved.

1. Introduction

Due to the major blackouts caused by voltage collapse [1], the voltage stability problem has become one of the most significant challenges in the planning and operation of the modern electric power systems. Voltage instability is usually characterized by an initial and progressive decrease in voltage magnitudes until a sharp rapid decline occurs; however, in some cases, the voltage magnitudes prior to undergoing the sharp change lie in a permissible range and the operators may observe no advance warning signal until large changes in the system state occurs [2]. Therefore, over the past several years, massive efforts have been devoted to the development of practical measures of the distance from the current operating state to the voltage collapse point, thereby providing an early warning of a critical situation.

Existing methods for voltage stability analysis are usually classified into static methods (such as PV curves and modal analysis), and dynamic methods (such as time domain simulation) [3]. The static approaches are based on the steady state power flow model

of the power systems and many aspects of voltage stability problems can effectively be analyzed using these methods; however, such simplified approaches usually lead to unreliable results as shown in [4]. In order to get a much more realistic picture of the voltage stability phenomena, it is necessary to take system dynamics into account. On the other hand, the application of dynamic methods may be too time-consuming for online use.

Using artificial neural networks (ANNs) would be an attractive alternative to overcome the aforementioned problems. ANNs are information processing systems inspired by the way biological neural systems process data. Application of neural networks to power system problems is an area of growing interest [5]. The main reasons are the ability of ANNs to learn complex non-linear relationships and their modular structures, which allows parallel processing [6].

Proposed methods in the past for online voltage stability monitoring using ANNs have led to acceptable results. As summarized in Table 1, the majority of the published works in the literature are based on the multi-layered perceptron (MLP) neural networks [7–14], while the other methods rely on the Radial Basis Function (RBF) networks [15–20].

The previously published approaches often require a large number of input variables [13,14,18]. Having a large number of inputs

* Corresponding author. Tel.: +98 131 6690274 8; fax: +98 131 6690271.

E-mail addresses: bahmanyar@iust.ac.ir (A.R. Bahmanyar), karami_al@yahoo.com, karami_s@guilan.ac.ir (A. Karami).

Table 1
Comparison of the proposed methods for voltage stability monitoring using ANNs.

Proposed method	ANN type	ANN inputs	ANN output(s)	Considering different system configurations	Employed method for feature selection
Method of Ref. [7]	MLP	Active and reactive line flows	VSM ^a	Separate ANNs for each configuration	Principal component analysis (PCA), Contingency analysis
Method of Ref. [8]	MLP	Bus net active and reactive powers and generators reactive power	Minimum energy margin	Separate ANNs for each configuration	Sensitivity analysis
Method of Ref. [9]	MLP	Load active and reactive powers	VSM	A separate ANN for each configuration	Regression-based sensitivity analysis
Method of Ref. [10]	MLP	Active and reactive line flows and bus voltages	VSM	A separate ANN for each configuration	Principal component analysis (PCA), K-means clustering
Method of Ref. [11]	MLP	Bus voltage magnitudes and phase angles	VSM	A single ANN for different configurations	Sequential forward selection
Method of Ref. [12]	MLP, Self-organizing map (SOM)	Bus voltage magnitudes, phase angles and injected active and reactive powers	VSM and real part of critical eigenvalues	A single ANN for different configurations or A separate ANN for each configurations	Self-organizing map (SOM) ANN
Method of Ref. [13]	MLP	Load buses voltage magnitude and active and reactive powers	VSM	A separate ANN for each specified bus	–
Method of Ref. [14]	MLP	Voltage magnitudes, active and reactive powers of generator and load buses	L-index	Two separate ANNs one for normal condition and the other for contingency conditions	–
Method of Ref. [15]	RBF	Voltage magnitude of PV buses and total system load	Probability of voltage collapse	–	–
Method of Ref. [16]	RBF	Load active and reactive powers	Voltage performance index	A separate ANN for each cluster of input pattern	Class separability index and Correlation conditions
Method of Ref. [17]	RBF	MVA flows in selected critical lines	VSM	A single ANN for different configurations	–
Method of Ref. [18]	RBF	Load active and reactive powers	VSM	A single ANN for different configurations	–
Method of Ref. [19]	RBF	Dominant features of the voltage profile extracted by wavelet transform	VSM	A single ANN for different configurations	Principal component analysis (PCA)
Method of Ref. [20]	RBF	Active and reactive line flows	L-index	A separate ANN for each configuration	Mutual information

^a VSM: The MW distance from the base operating point to the critical collapse point.

not only increases the size of the ANN, but also raises the cost as well as the time required for future data collection. In this paper, a fast and efficient method for reducing the number of input variables is proposed. Here, the Gram–Schmidt orthogonalization process is first employed to reduce the number of input variables, and then the neural network-based sensitivity technique proposed in [21] is used to find the minimum number of features required to make a good estimation of a voltage stability margin (VSM). The VSM is defined as the distance from the current operation state to the maximum voltage stability limit point (voltage collapse point) according to the system loading parameter.

In practice, a power system may face with a wide range of contingencies during its actual operating conditions such as unexpected line outages. When a contingency takes place, the system topology (configuration) changes and the trained ANN may fail to provide an accurate estimate of the VSM as it would be unable to capture the input–output relationship properly. Research works presented in [7–9,20], employ a separate ANN to estimate the VSM for each system configuration (contingency). For a large power system, with a huge number of potentially credible contingencies, training a separate ANN for each resulting configuration would be a demanding task. Therefore, in the present study, all single line outages are analyzed and ranked in descending order in terms of their VSMs and then a single MLP ANN is employed to estimate the VSM for the base case operating conditions and for a selected number of the worst case contingencies.

The proposed online voltage stability monitoring scheme is applied to the New England 10-machine, 39-bus test power system and the simplified southern/eastern (SE) Australian power system, considering high order dynamic models for the generators along

with their automatic voltage regulators (AVRs). Since the voltage collapse phenomenon is highly affected by reactive power generation limits of the synchronous machines [22], the reactive power generation limits are also imposed in this paper. The MATLAB-based free and open source software tool PSAT (*Power System Analysis Toolbox*) [23] is used in this paper to obtain the required training and/or testing patterns for the ANNs by performing the continuation power flow (CPF) method on both test systems, whereas the proposed neural network models are implemented in MATLAB.

The rest of the paper is organized as follows: the use of VSM for voltage stability monitoring is described in Section 2. Section 3 gives an introduction to the MLP neural networks and presents the methodology of the proposed method. Section 4 describes the employed method for selecting the worst case contingencies. Details of the method used for reducing the number of input features are explained in Section 5. Case studies are given in Section 6, and finally, Section 7 concludes the paper.

2. Voltage stability margin

Voltage instability results from the attempts of loads to draw more power than can be delivered by the transmission and generation systems [24]. Suppose that a sample power system is operating stably at a certain loading level. Fig. 1 shows the variation of the voltage magnitude of a particular load bus in the system against a loading parameter λ , representing an independent system parameter that is slowly varied, such as active and reactive loads and/or active generation dispatch. For the system loading below

the maximum, there are two solutions, one with higher voltage (stable), and the other with lower voltage (unstable). As the system loading increases following a certain direction, these solutions approach each other and finally coalesce at a critical point. This nose point or saddle-node bifurcation (SNB) point corresponds to the maximum transmissible power [25]. Increasing the system loading beyond this point could lead the entire system to voltage collapse.

In this paper, the voltage stability margin (VSM) is defined as the distance from the current operating state to the voltage collapse point according to the system loading parameter; therefore, as illustrated in Fig. 1, for calculating this margin, the SNB point should be located.

As reported in the literature, the SNB point can be identified using either direct or continuation methods [26–28]. Direct methods find this point by solving an augmented system of equations. These methods have been shown to be efficient and accurate in locating the saddle node bifurcation points [26,28]; however, they need a good initial guess and may fail if all the system limits are considered [28].

Continuation methods, by contrast, do not have the mentioned limitations and also provide more information. Starting from an initial point, these methods trace the equilibrium points of a power system state as its parameters change in a quasi-continuous manner. Continuation methods are robust and accurate, but they are computationally expensive, especially for large power systems [28,29]. Artificial neural networks provide an attractive alternative to overcome the problem of computational burden of the continuation algorithms, since after training, an ANN can estimate its outputs very fast due its parallel architecture.

3. Artificial neural network design

An artificial neural network is an information processing system that has certain performance characteristics in common with biological neural networks [30]. In this study, a multi-layered feedforward neural network topology is employed. This network, also called multi-layered perceptron (MLP), is the most popular neural network in use today. An MLP neural network consists of one input layer, one output layer and one or more hidden layers. The number of neurons in the input and output layers are, respectively, equal to the number of inputs and outputs, while a trial-and-error procedure is usually employed to determine the number of neurons in the hidden layers. Each neuron is connected to other neurons through communication links, each with an associated weight. The weights represent information being used to solve a problem and have to be determined by a learning (training) algorithm

[30]. The MLP neural networks are usually trained in a supervised manner with a highly popular algorithm known as the error back-propagation [31]. This algorithm is simply a gradient descent-based method to minimize the total squared error of the output computed by the net. However, the conventional back-propagation method is often too slow for many practical problems; thus, in this paper the *resilient* back-propagation technique, which is one of the fast training algorithms, is employed to accelerate the training process. This training algorithm is thoroughly described in [32].

3.1. Selection of input variables

Proper selection of the input variables is a crucial factor for the success of neural networks. Almost all voltage collapse incidents have occurred in heavily loaded systems. Furthermore, research has shown that voltage stability is strongly influenced by system loads [33,34]. On the other hand, synchronous generators are a primary source of the reactive power and are to a great extent, responsible for maintaining a good voltage profile across the power system [24]; therefore, the following seems to be a suitable set of input variables for predicting the VSM:

- Voltage magnitudes and generated active powers of the PV buses.
- Active and reactive powers of all the system loads.
- Generated reactive powers of all the system generators.
- Generated active power of the slack bus.

3.2. Generation of training patterns

In both test systems used in this paper, for generating training and/or testing patterns of the MLP ANNs, active and reactive powers of all system loads as well as voltage magnitudes of PV buses are varied randomly within specified ranges of their base case values. Here, it is assumed that the range of variations of the voltage magnitudes of all the PV buses is bounded from 0.9 to 1.1 times their corresponding base case values. It is further assumed that both real and reactive loads at all buses vary in the range of 0.7 to 1.2 times their corresponding base values, according to the following relations:

$$\begin{aligned} V_{PV_{i0}}(k) &= V_{PV_{ib}}(0.9 + 0.2\varepsilon_{V_{PV}}^i(k)) \\ P_{L_{i0}}(k) &= P_{L_{ib}}(0.7 + 0.5\varepsilon_{P_L}^i(k)) \\ Q_{L_{i0}}(k) &= Q_{L_{ib}}(0.7 + 0.5\varepsilon_{Q_L}^i(k)) \end{aligned} \quad (1)$$

where $P_{L_{i0}}(k)$, $Q_{L_{i0}}(k)$ and $V_{PV_{i0}}(k)$ are, respectively, the load active power, load reactive power and the PV bus voltage magnitude at the i th bus for the k th training pattern. Also, $P_{L_{ib}}$, $Q_{L_{ib}}$, and $V_{PV_{ib}}$ denote, respectively, the base case load active power, load reactive power and the PV bus voltage magnitude at the i th bus, and ε denotes a uniformly distributed random number within [0,1]. All the system loads are modeled as constant power loads and load changes are picked up by all the system generators based on their base case generated active powers. Each randomly generated set of operating conditions is then verified by a conventional power flow program to make sure that each of the cases provides a feasible power flow solution. The cases, for which the power flow does not meet the steady state operating requirements, are removed.

For each verified operating point, the voltage stability margin is then calculated using a continuation power flow method. During this continuation process, the real and reactive powers of all system loads are increased maintaining their power factors fixed as in the base case loading condition. Each generator is assigned a participation factor of the load demand based on its initial generated active power and the parameter λ is used to simulate the

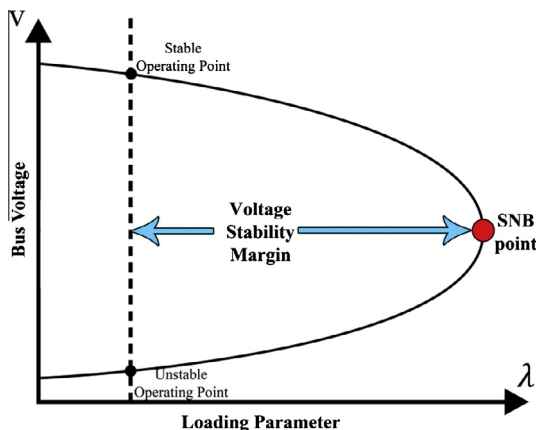


Fig. 1. Illustration of the voltage stability margin (VSM).

active and reactive power load increases throughout the system as follows:

$$\begin{aligned} P_{L_i}(\lambda) &= P_{L_{i0}}[1 + \lambda] \\ Q_{L_i}(\lambda) &= Q_{L_{i0}}[1 + \lambda] \\ P_{G_i}(\lambda) &= P_{G_{i0}}[1 + \lambda K_{G_i}] \end{aligned} \quad (2)$$

where K_{G_i} is the distributed slack bus variable. The VSM is defined as the distance from the base case operating point to the voltage collapse point according to the system loading parameter λ . The VSM is expressed by:

$$\text{VSM} = \frac{|S_M| - |S_0|}{|S_0|} \quad (3)$$

where $|S_M|$ and $|S_0|$ denote the maximum and the base case values of the total system apparent power consumed, respectively. For a power system with n buses, the voltage stability margin can be calculated as:

$$\text{VSM} = \frac{|S_M| - |S_0|}{|S_0|} = \frac{\sum_{i=1}^n \sqrt{P_{L_{i\max}}^2 + Q_{L_{i\max}}^2} - \sum_{i=1}^n \sqrt{P_{L_{i0}}^2 + Q_{L_{i0}}^2}}{\sum_{i=1}^n \sqrt{P_{L_{i0}}^2 + Q_{L_{i0}}^2}} \quad (4)$$

Using (2), $P_{L_{i\max}}$ and $Q_{L_{i\max}}$ are obtained by:

$$\begin{aligned} P_{L_{i\max}} &= P_{L_{i0}}[1 + \lambda_{\max}] \\ Q_{L_{i\max}} &= Q_{L_{i0}}[1 + \lambda_{\max}] \end{aligned} \quad (5)$$

where $P_{L_{i\max}}$ and $Q_{L_{i\max}}$ denote the maximum load active power and the maximum load reactive power at the i th bus, respectively. Also, λ_{\max} shows the maximum system loading parameter. Putting $P_{L_{i\max}}$ and $Q_{L_{i\max}}$ from (5) into (4), one can easily show that the VSM is indeed equal to λ_{\max} . In other words, we have:

$$\text{VSM} = \lambda_{\max} \quad (6)$$

Therefore, the calculated VSM is used as the target output for the training and/or testing patterns. The above procedure is repeated to generate a sufficient number of training and/or testing patterns for the proposed neural network. Fig. 2 shows the overall steps used for the ANN pattern generation.

4. Contingency analysis

A power system is subjected to a wide range of disturbances during its actual operating conditions, and the occurrence of a disturbance is sometimes followed by removal of the faulted element resulting in a new system configuration; therefore, it is essential for the trained ANN to be able to estimate the VSM for different system configurations. One simple idea is to train a separate ANN for each considered topology. This method is shown to have promising results [7–9,20]; however, using this approach in a practical system requires the knowledge of the post-contingency system configuration. Furthermore, for a large power system, with a huge number of potentially credible contingencies, training a separate ANN for each resulting configuration would be a demanding task. In this paper, a single ANN is trained for several system configurations.

The security of the power system is commonly defined based on the single contingency ($N-1$) criterion, meaning normal system minus one element. However, it is impractical and unnecessary to train the neural network for all possible contingencies; therefore, contingencies should be ranked using a suitable voltage stability criterion to identify the most critical situations under voltage collapse point of view. The margin between the current operating point and the voltage collapse point is the most commonly used index for voltage stability analysis and the majority of the proposed contingency analysis methods in the literature,

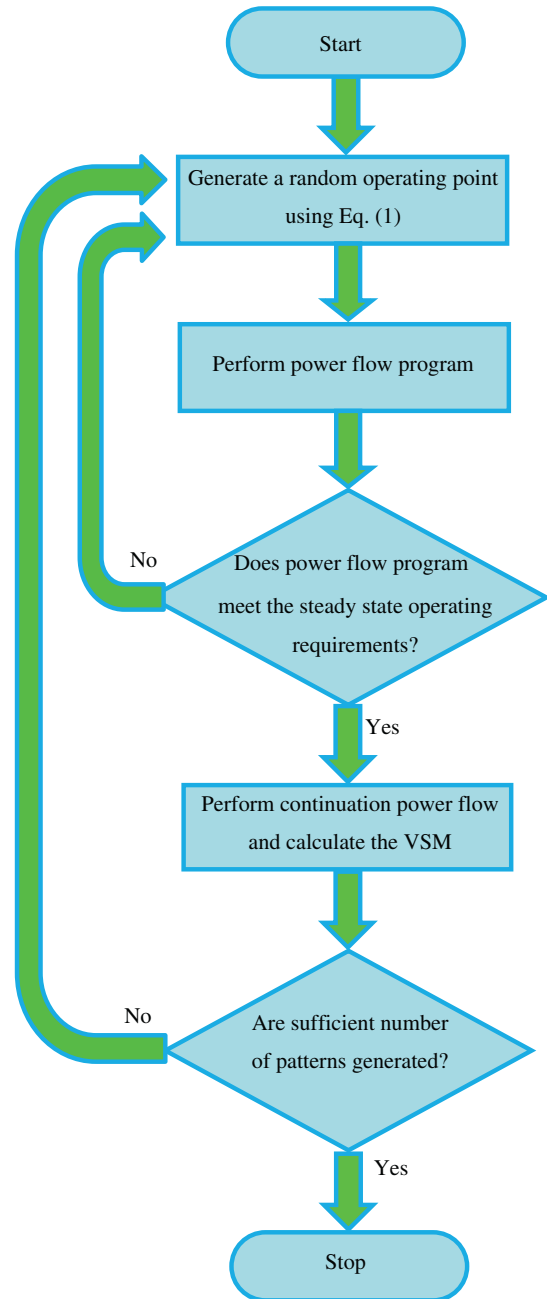


Fig. 2. Steps used for neural network pattern generation.

are based on this index [35,36]. In the present study, all single line outages are first analyzed and ranked in descending order in terms of their VSMs, and then a single neural network is trained to estimate the VSM for the base case operating conditions and for a selected number of the worst case contingencies.

5. Reduction of input variables

Power system measurements are very redundant and the number of variables is extremely high. Thus, restricting the input space to a small subset of the available input variables has obvious economic benefits in terms of data storage, computational requirements and cost of future data collection [37]; furthermore, reducing the number of input variables leads to better model understanding in some cases. The optimal input variable set will contain the fewest input variables required to describe the

behavior of the output target, with a minimum degree of redundancy and with no uninformative variables [38]. One simple approach to find the optimal subset is to evaluate all possible combinations of the input variables. This approach may be feasible when the dimension of the input set is low, but as the dimension increases, it becomes unfeasible. There are a wide variety of methods for selecting a reduced number of input features. A simple method, particularly useful in practice, is the Gram–Schmidt orthogonalization process. This method is a forward selection algorithm which ranks the input set by adding progressively features, which correlate to the target in the space orthogonal to the already selected features [37].

Let column $X_k = [x_{k1}, x_{k2}, \dots, x_{kM}]^T$ denote the values taken by the k th feature for all patterns, in which there are M patterns. Also, suppose that $Y = [y_1, y_2, \dots, y_M]^T$ is the vector of calculated values for the target output. In each cycle of the Gram–Schmidt process, the following correlation coefficients need to be computed [39]. These coefficients determine the strength of relationship between the input features and the target output:

$$\cos^2(X_k, Y) = \frac{(X_k \cdot Y)^2}{\|X_k\|^2 \|Y\|^2}, k = 1, \dots, N \quad (7)$$

where N is the total number of features, and $(X_k \cdot Y)$ defines the inner product between the vectors X_k and Y . Also, $\|\cdot\|^2$ denotes the second norm.

As depicted in Fig. 3, in the first iteration, the vector X_k for which the correlation coefficient given by Eq. (7) is the biggest is selected as the most relevant feature. The remaining candidate inputs and the output vector are then projected into the subspace (of the dimension $N-1$) of the selected feature to discard the part of the concept that is explained by the first selected vector. Then, in the next iteration, the most relevant projected feature is selected among those features not selected in the previous iteration, and the $N-2$ remaining features are projected into the subspace of the first two ranked vectors. Finally, when all the N input vectors are ranked, the algorithm terminates.

After ranking the input variables by the above procedure, the fewest input features, required to describe the behavior of the output of the ANN are selected. Furthermore, to make sure that those selected features are indeed the most relevant ones, the influence of each of them on the training process of the ANN is examined through the neural network-based sensitivity technique proposed in [21]. The irrelevant features are then removed from the reduced input set. The algorithm is computationally efficient and tends to result in the selection of relatively small set of input features.

6. The simulation results

The New England 10-machine 39-bus test system [40] and the simplified southern/eastern (SE) Australian power system [41], with high order dynamic models for the synchronous generators along with their AVR are used here to demonstrate the proposed scheme for online voltage stability monitoring. Generators reactive power limits are known as the key factors that greatly affect the voltage stability [42]; therefore, the generators reactive power limits are also imposed in this paper. The MATLAB-based free and open source software tool PSAT [23] along with its source codes are employed to find the voltage stability margin by using the continuation power flow (CPF) method on both test systems.

For each test system, a single ANN is trained to estimate the VSM for the base case operating conditions and for a selected number of the worst case contingencies. In order to examine the generalization capability of the proposed neural networks, the root mean-squared error (RMSE) between the actual VSM and the esti-

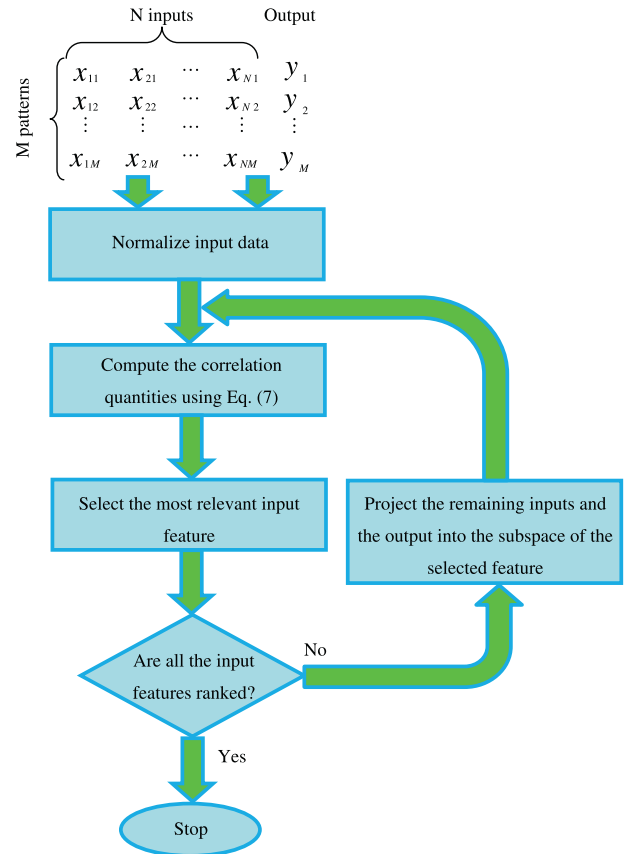


Fig. 3. The Gram–Schmidt orthogonalization process.

ated VSM by the trained ANN is calculated. This performance measure is defined as follows:

$$\text{RMSE} = \sqrt{\frac{1}{NP} \sum_{p=1}^{NP} (\text{actual VSM}(p) - \text{estimated VSM}(p))^2} \quad (8)$$

where p represents the pattern number, and NP denotes the total number of patterns in the corresponding set (training or testing). The neural network toolbox of MATLAB, Mathworks Inc., is used for training the proposed MLP ANNs [43]. All the computations are performed on a personal computer with 2-GHz Intel Core 2 Duo processor and 2 GB of RAM running MATLAB 7.8.

6.1. The simulation results for the New England 39-bus test system

The single-line diagram of the New England 10-machine 39-bus test system is shown in Fig. 4. The bus and line data of the system can be found in [40]. This system consists of 29 PQ buses, 46 lines and 10 synchronous machines equipped with IEEE type-1 voltage regulators. All machines are presented by their 4th order dynamic model. Only 19 buses in the system have nonzero real and reactive loads that were modeled as constant power loads. Bus 1 was taken as the slack bus and its voltage magnitude and angle were assumed to be fixed. The remaining generator buses (i.e., buses 2–10) were taken as the PV buses having specified voltage magnitudes and generated active powers. Based on the explanations mentioned in Section 3.1, the following system operating conditions were selected as the initial input variables for an MLP ANN to estimate the VSM in the New England 39-bus system:

- Voltage magnitudes and generated active powers of all 9 PV buses.
- Active and reactive powers of all 19 system loads.

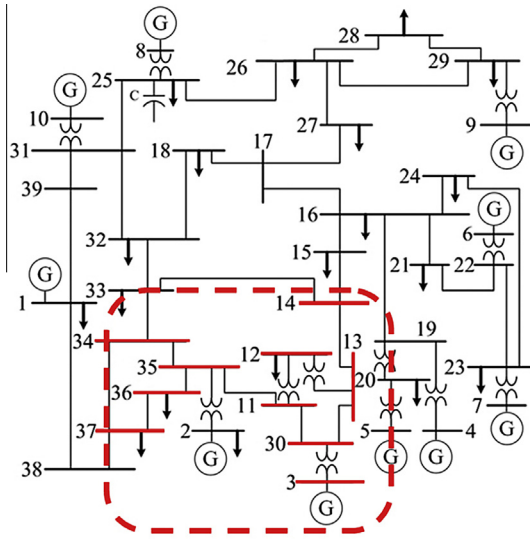


Fig. 4. Single-line diagram of the New England 39-bus test system.

- Generated reactive powers of all 10 system generators.
- Generated active power of the slack bus.

Therefore, the proposed neural network architecture has 67 $(9 + 9 + 19 + 19 + 10 + 1)$ inputs, while its output is the voltage stability margin.

As mentioned before, we want to estimate the VSM for both the base case configuration and for a selected number of severe contingencies. To identify the most severe contingencies, contingency analysis was carried out for all single line outages in the New England 39-bus system, and then five contingencies were selected as the most critical ones. The selected contingencies along with their corresponding VSMs in the base case loading condition are shown in Table 2. Therefore, our aim here is to estimate the VSM for a total of six system configurations, i.e., for the base case plus five severe configurations. The CPF method was then employed to obtain the required training and/or testing patterns for the ANN.

Table 2
Set of the selected contingencies for the New England 39-bus test system.

Contingency no.	Description	VSM
1	Outage of the line between bus 15 and bus 16	0.2600
2	Outage of the line between bus 32 and bus 33	0.2936
3	Outage of the line between bus 37 and bus 38	0.3080
4	Outage of the line between bus 21 and bus 22	0.3082
5	Outage of the line between bus 31 and bus 32	0.3086
Base case	All transmission lines are in service	0.3644

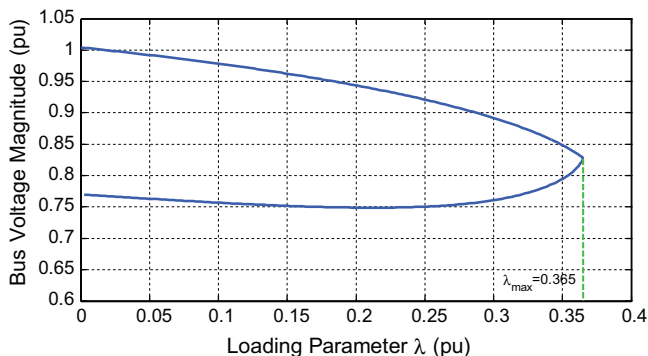


Fig. 5. Voltage magnitude versus loading parameter (λ) curve for bus-12 in the New England 39-bus test system.

As an example, Fig. 5 shows the complete PV curve for bus-12 in the New England 39-bus test system produced by the PSAT, which employs the CPF method. In this figure, the variation of bus-12 voltage magnitude against the system loading parameter is plotted. Here, $\lambda = 0$ corresponds to the base case loading condition; as the system loading increases, the bus voltage decreases and system equilibrium points approach to the nose point of the curve. As can be seen in Fig. 5, the voltage stability margin (i.e., λ_{\max}) for the base case loading condition in the New England 39-bus test system is therefore equal to 0.365 p.u.

Using the procedure described in Section 3.2, 950 random patterns were generated for each of the above-mentioned six system configurations, from which 750 patterns were chosen as the training patterns and the remaining 200 patterns were chosen as the testing patterns for the proposed MLP ANN. Therefore, a total amount of 4500 $(6 * 750)$ patterns were collected as the training patterns, and a total amount of 1200 $(6 * 200)$ as the testing patterns to estimate the VSM considering multiple configurations using a single MLP ANN in the New England 39-bus test system. Before training, the input and output data patterns were scaled so that they fell in the range $[-1, 1]$.

Two cases were considered for training the proposed ANN. In the first case, all the above-mentioned 67 variables were used as the ANN inputs; while in the second case, training was performed using a reduced set of input variables. Results obtained for both cases are described below.

6.1.1. Training the ANN using all inputs in the New England system

To train an MLP ANN, we need to choose a proper structure for the neural network along with suitable activation functions for its neurons. Here, after several trials an MLP neural network with one input layer consisting of 67 inputs, one hidden layer including 8 neurons, and one output layer was employed to estimate the VSM for the multiple configurations in the New England 39-bus test system. Moreover, hyperbolic tangent transfer functions were chosen for the hidden layer neurons and a linear transfer function was used for the output neuron.

In Table 3, the error goal, the Mean-Squared Error (MSE) between the actual VSM and the estimated VSM in the training phase along with the RMSE obtained for the testing patterns are given. The proposed MLP ANN was trained using the *resilient* back-propagation method, which is one of the fastest techniques for training large neural networks. It took about 2.15 s with 48 epochs on average to train the proposed MLP ANN. It should be noted that other fast training algorithm, such as Levenberg–Marquardt could be employed to train the proposed MLP ANN [44].

As can be seen in Table 3, the proposed MLP ANN could estimate its target (i.e., the VSM) with a very small RMSE value for the testing patterns, proving the generalization accuracy of the trained MLP ANN for the New England 39-bus test system. To see this better, the estimated VSM and the corresponding actual VSM in the New England 39-bus are compared in Fig. 6, for 20 out of 1200 testing patterns due to limited space. It is observed from this figure that the trained MLP ANN has estimated the actual VSM with reasonable accuracy under different system configurations as well as operating conditions. Moreover, in comparison to CPF method which takes about 2 s to calculate the VSM, the trained ANN estimates this margin almost instantaneously.

6.1.2. Training the ANN using the reduced set of inputs in the New England system

The results obtained in Section 6.1.1 confirmed that for the New England 39-bus test system, the VSM could be estimated using an MLP ANN with 67 inputs with reasonable accuracy. However, there are redundant variables that do not bring new information into the model. Using the Gram–Schmidt orthogonalization process

Table 3
Summary of the neural networks training results for the New England 39-bus system.

Case no.	Neural network output	Number of inputs	Number of hidden neurons	MSE for training patterns	RMSE for testing patterns
1	VSM	67	8	0.005	0.0190
2	VSM	5	8	0.005	0.0196

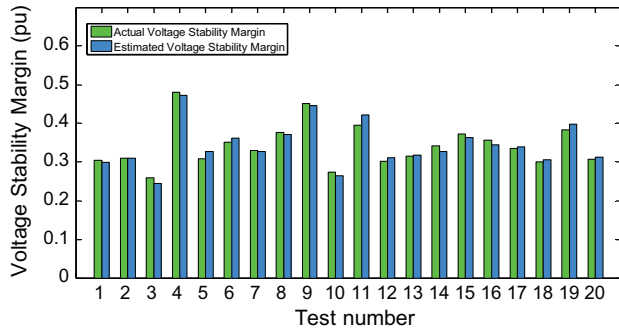


Fig. 6. Comparison of ANN estimated VSM and the corresponding actual VSM for different configurations of the New England system using all input variables.

described in Section 5, the above-mentioned 67 input variables were ranked, and then 7 variables were selected as the important features to train another MLP ANN to estimate the VSM. In addition, the ANN-based sensitivity technique described in [21] was employed to obtain the final reduced features among those 7 variables selected by the Gram–Schmidt orthogonalization procedure.

To perform that ANN-based sensitivity technique, each of the 7 mentioned features is removed from the inputs one at a time, and an MLP neural network using the remaining 6 features is trained with the same 4500 training patterns as used in Section 6.1.1. The relevant features would then be those features that removing each of them from the neural network inputs, makes the neural network a long time to converge. In addition, the testing results of the newly trained network would be very poor for the case of important features. In other words, for a given selected feature set, the inclusion of one of the remaining features would increase the performance of the trained neural network if it were a salient one.

Employing that ANN-based sensitivity technique, 5 out of 7 features were identified as the most relevant features for training the proposed MLP ANN. The features were as follows:

- Generated reactive power of the generator at bus 3.
- Voltage magnitudes at buses 2, 3 and 4.
- Generated active power of the slack bus.

The question that now arises is why the above selected features are the most relevant ones. To address this issue, we need to identify the weakest buses in the New England test system. As shown in [29], since the tangent vector, which is defined as $dV/d\lambda$, converges to the zero right eigenvector at the bifurcation point, hence the largest entries on this vector correspond to the buses that are critical to maintain voltage stability. Therefore, identifying the weakest buses is as easy as choosing the buses that has the largest differential changes in the voltage magnitude dV , at the bifurcation point. The 10 weakest buses identified via this tangent vector approach are specified in Fig. 4. As shown in this figure, generators at bus 2 and bus 3 are indeed the nearest machines to the critical area in the New England 39-bus test system; this means that, if the system loading increases further, they are more prone to voltage collapse. Therefore, the generated reactive powers and voltage magnitudes of these buses are very informative input variables.

The generated active power of the slack bus also contains some important information regarding the base case generated active power and transmission losses; therefore, this feature is chosen as one of the most relevant input variables as well. The aforesaid reasoning not only answers the above question but also confirms the effectiveness of the proposed method.

Another MLP ANN was employed to estimate the VSM in the New England 39-bus test system with the same 4500 training patterns as in Section 6.1.1, using the above-mentioned 5 features as the ANN inputs and the VSM as its output. Here, the employed MLP ANN architecture was the same as that used in Section 6.1.1. The proposed MLP ANN was again trained using the resilient back-propagation method. It took about 3.18 s with 153 epochs on average to train the proposed MLP ANN. The error goal, the MSE between the actual VSM and the estimated VSM in the training phase along with the RMSE obtained for testing patterns of the trained MLP, are also shown in Table 3.

As can be seen in Table 3, the proposed MLP ANN could estimate its target with a very small RMSE value for the testing patterns. The estimated VSM and the corresponding actual VSM in the New England 39-bus system using those selected 5 features as the ANN inputs are compared in Fig. 7, for 20 out of 1200 testing patterns. As illustrated in this figure, the trained MLP ANN has again estimated the VSM with reasonable accuracy under different system configurations as well as operating conditions. In comparison to the case of Section 6.1.1, the neural network training time has increased and its prediction accuracy has decreased here; however, reducing the number of inputs to just 5 features has resulted in a compact and efficient ANN model in this case.

6.2. The simulation results for the simplified model of SE Australian power system

Fig. 8 shows the single-line diagram of the southern/eastern (SE) Australian power system. This system consists of 28 PQ buses, 164 transmission lines and 14 power stations of 2 to 12 units. All the system generators are represented by their 4th order dynamic models and are equipped with different excitation systems according to the data provided in [41]. Only 28 buses in the system have nonzero real and reactive loads. All the system loads were modeled as the constant powers. Bus 204 was taken as the slack bus and its

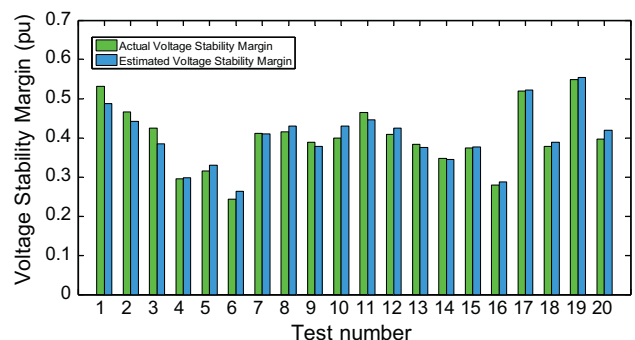


Fig. 7. Comparison of ANN estimated VSM and the corresponding actual VSM for different configurations of the New England system using the reduced input variables.

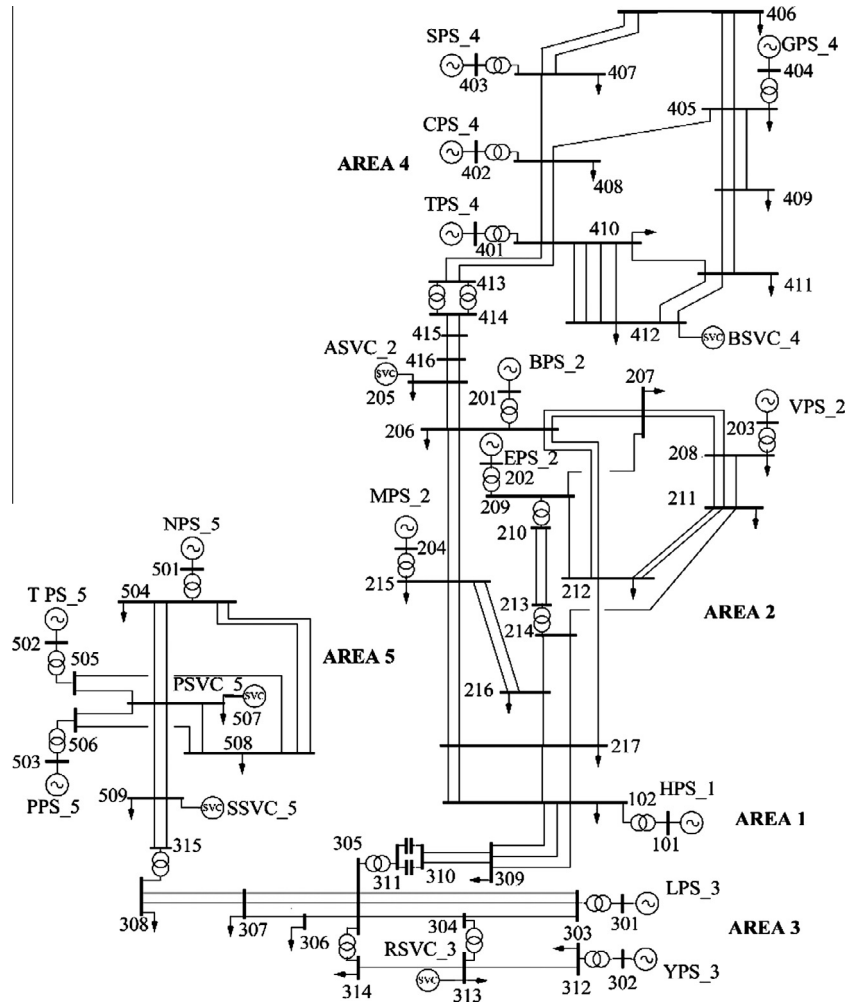


Fig. 8. Single-line diagram of the southern/eastern (SE) Australian power system.

voltage magnitude and voltage angle were assumed to be fixed. The remaining 13 generator buses were taken as the PV buses having specified voltage magnitudes and generated active powers. The system also has 5 static VAR compensators (SVCs), 4 shunt capacitors, and 3 shunt reactors. Here, the following system operating conditions were selected as the initial input variables for an MLP ANN to estimate the VSM in the SE Australian power system:

- Voltage magnitudes and generated active and reactive powers of all 13 PV buses.
- Active and reactive powers of all 28 system loads.
- Generated active and reactive powers of the slack bus.
- Generated reactive powers of 5 SVCs, 4 shunt capacitors, and 3 shunt reactors.
- Voltage magnitudes of 5 buses at which the SVCs are connected.

Thus, the proposed ANN has 114 ($13 + 13 + 13 + 28 + 28 + 2 + 5 + 4 + 3 + 5$) inputs, while its output is the voltage stability margin.

Similar to the previous test system, here we want to estimate the VSM for both the base case configuration and for a selected number of severe contingences. Contingency analysis was again carried out for all the single line outages in the SE Australian power system to identify the most sever contingences, and then seven contingences were chosen as the most critical ones. The selected contingences and their corresponding VSMs are shown in Table 4.

Our aim here is to estimate the VSM for the base case and for the seven severe configurations. In addition, The CPF method was again employed to obtain the required training and/or testing patterns for the VSM.

As an example, Fig. 9 shows the complete PV curve for bus-409 in the SE Australian power system, produced by PSAT that employs the CPF method. The figure shows the variation of bus-409 voltage magnitude against the system loading parameter. Here, $\lambda = 0$ corresponds to the base case loading condition; as the system loading increases, the bus voltage decreases and the system equilibrium points approach to the nose point of the curve. As is evident from Fig. 9, the voltage stability margin (i.e., λ_{\max}) for the base case loading condition in the SE Australian power system is equal to 0.37 p.u.

Using the procedure described in Section 3.2, 950 random patterns were generated for each of the above-mentioned eight system configurations, from which 750 patterns were chosen as the training patterns and the remaining 200 patterns, were chosen as the testing patterns. Therefore, a total amount of 6000 ($8 * 750$) patterns were used as the training patterns, and 1600 ($8 * 200$) patterns as the testing patterns to estimate the VSM considering multiple configurations using a single MLP ANN. Here, it was assumed that the variations of the voltage magnitudes of the SVC buses are bounded from 0.9 to 1.1 times their corresponding base case values. Before training, the input and output data patterns were scaled so that they fell in the range $[-1, 1]$.

Table 4
Set of the selected contingencies for the SE Australian power system.

Contingency no.	Description	VSM
1	Outage of the line between bus 408 and bus 410	0.1733
2	Outage of the line between bus 303 and bus 304	0.1957
3	Outage of the line between bus 303 and bus 305	0.2077
4	Outage of the line between bus 405 and bus 409	0.2726
5	Outage of the line between bus 307 and bus 308	0.2870
6	Outage of the line between bus 409 and bus 411	0.3079
7	Outage of the line between bus 410 and bus 411	0.3144
Base case	All transmission lines are in service	0.3701

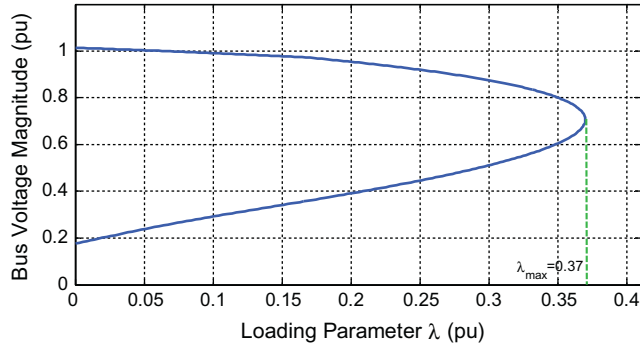


Fig. 9. Voltage magnitude versus loading parameter (λ) curve for bus-409 in the SE Australian power system.

Similar to the pervious test system, two cases were considered for training the proposed ANN in the SE Australian power system. In the first case, all the above-mentioned 114 variables were used as the ANN inputs; while in the second case, training was performed using a reduced set of input variables.

6.2.1. Training the ANN using all inputs in the SE Australian system

As mentioned before, to train an MLP ANN, a proper structure for the neural network along with suitable activation functions for its neurons should be determined. Here, after several trials an MLP neural network with one input layer consisting of 114 inputs, two hidden layers including 12 and 8 neurons each, and one output neuron was employed to estimate the VSM for the selected configurations in the SE Australian power system.

In Table 5, the error goal, the Mean-Squared Error (MSE) between the actual VSM and the estimated VSM in the training phase along with the RMSE obtained for the testing patterns are given. The resilient back-propagation method was again used to train the proposed MLP ANN. It took about 8.1 s with 132 epochs on average to train the proposed MLP ANN.

As can be seen in Table 5, the proposed MLP ANN could estimate its target (i.e., the VSM) with a very small RMSE value for the testing patterns, proving the generalization accuracy of the trained MLP ANN for the SE Australian power system. To ease comparison, the estimated VSM and the corresponding actual VSM are compared in Fig. 10 for 20 out of 1200 testing patterns. As shown in

Table 5
Summary of the neural networks training results for the SE Australian power system.

Case no.	Neural network output	Number of inputs	Number of first hidden layer neurons	Number of second hidden layer neurons	MSE for training patterns	RMSE for testing patterns
1	VSM	114	12	8	0.01	0.047
2	VSM	11	12	8	0.01	0.035

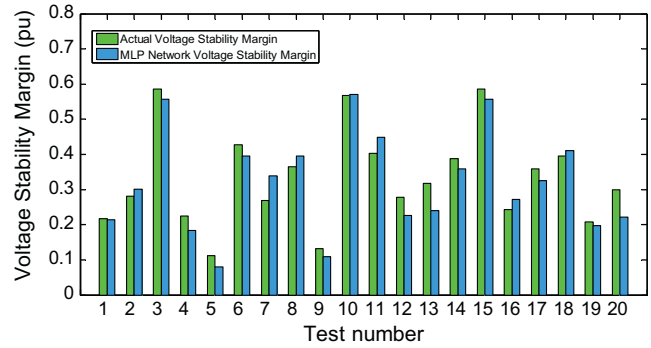


Fig. 10. Comparison of ANN estimated VSM and the corresponding actual VSM for different configurations of the SE Australian power system using all input variables.

this figure, the trained MLP ANN has estimated the actual VSM with reasonable accuracy under different system configurations as well as operating conditions. Moreover, in comparison to CPF method which takes about 4 s to calculate the VSM for the SE Australian power system, the trained ANN estimates this margin almost instantaneously.

6.2.2. Training the ANN using the reduced set of inputs in the SE Australian system

The results obtained in Section 6.2.1 indicated that the VSM for the SE Australian test system could be estimated fairly accurately by using an MLP ANN with 114 inputs. However, as stated earlier, there are redundant variables that do not bring new information into the model. Therefore, the above-mentioned 114 input variables were ranked using the Gram–Schmidt orthogonalization process, and then 15 variables were selected as the important features. Furthermore, the ANN-based sensitivity technique described in [21] was again employed to obtain the final reduced features among those 15 variables selected by the Gram–Schmidt orthogonalization process.

Employing that ANN-based sensitivity technique, 11 out of 15 features were identified as the most relevant features for training the proposed MLP ANN. The features were as follows:

- Generated reactive power of the generator at bus 301.
- Voltage magnitudes at the buses 302, 401, 404 and 509.
- Generated reactive power of the shunt capacitor at bus 409.
- Generated reactive powers of the SVCs at buses 313, 412, 507, and 509.
- Reactive power of the load at bus 409.

Using a similar reasoning as that mentioned in Section 6.1.2 for New England 39-bus test system, it could be verified that the above selected features are indeed the most important features. Therefore, another MLP ANN was employed to estimate the VSM in the SE Australian power system with the same 6000 training patterns as in Section 6.2.1, using the above-mentioned 11 features as the ANN inputs and the VSM as its output. Here, the employed MLP ANN architecture was the same as that used in Section 6.2.1. The resilient back-propagation method was again used for training

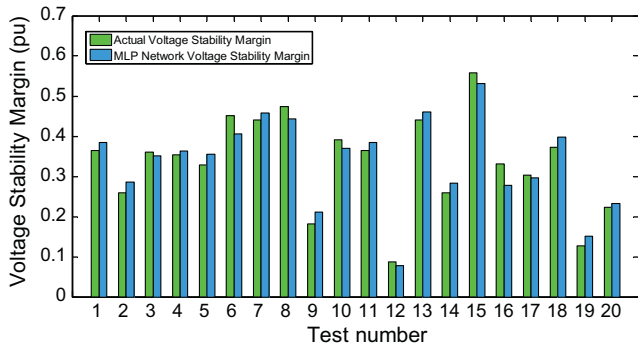


Fig. 11. Comparison of ANN estimated VSM and the corresponding actual VSM for different configurations of the SE Australian power system using the reduced input variables.

the proposed MLP NN. It took about 10.5 s with 261 epochs on average to train the proposed MLP ANN. In Table 5, the error goal, the MSE between the actual VSM and the estimated VSM in the training phase and the RMSE obtained for the testing patterns for the trained MLP ANN are also shown.

As can be seen in Table 5, the proposed MLP ANN could estimate its target (i.e., the VSM) with a very small RMSE value for the testing patterns, proving the generalization accuracy of the trained MLP ANN for the SE Australian power system. The estimated VSM and the corresponding actual VSM in the SE Australian power system with those selected 11 features as the ANN inputs are compared in Fig. 11 for 20 out of 1200 testing patterns. It is evident from this figure that the trained MLP ANN has estimated the actual VSM with reasonable accuracy under different system configurations as well as operating conditions. In comparison to the case of Section 6.2.1, the neural network training time has slightly increased here; however, its prediction accuracy has improved significantly. Therefore, removing the redundancy between variables has resulted in better estimation of the VSM by the trained MLP ANN.

7. Conclusions

Nowadays, voltage stability problem has become a major concern for the power system planners and operators. In online applications, system operators must be able to quickly recognize the potentially dangerous situations leading to voltage collapse to take the required remedial actions. Therefore, online voltage stability monitoring is becoming an important part of the modern day energy management systems (EMS). Furthermore, employing numerical simulation techniques to monitor the voltage stability status of a power system is computationally expensive even by using today's modern computers. To cope with these problems, in this paper, an artificial neural network (ANN)-based approach was presented for online estimation of a voltage stability margin (VSM). Unlike many of the previously published works, which employed a separate ANN for different contingencies, a new scheme for online estimation of the VSM for several system configurations by using only one ANN was presented in this paper. In addition, based on the Gram–Schmidt orthogonalization process and an ANN-based sensitivity technique, a systematic way of selecting the fewest system features as the neural networks inputs, was presented.

Numerical results were obtained on the New England 10-machine 39-bus test system and the SE Australian system by using high order dynamic models for the generators along with their automatic voltage regulators (AVRs), and by imposing their reactive power generation limits. Using the proposed feature selection

algorithm, the number of the ANN inputs was reduced to less than 10% of the initially selected features in both test systems. The results obtained confirmed that reducing the number of ANN inputs, not only has some obvious benefits in terms of the computational requirements as well as cost of the future data collection, but also could improve the generalization accuracy of the trained neural network.

Acknowledgement

The authors acknowledge the support of University of Guilan, Iran.

References

- [1] Taylor CW. Power system voltage stability. New York: McGraw-Hill; 1994.
- [2] Chiang HD, Dobson I, Thomas RJ. On voltage collapse in electric power systems. *IEEE Trans Power Syst* 1990;5(2):601–16.
- [3] Acharjee P. Identification of maximum loadability limit and weak buses using security constraint genetic algorithm. *Int J Electr Power Energy Syst* 2012;36:40–50.
- [4] Padma Subramanian D, Kumudini Devi RP, Saravanaselvan R. A new algorithm for analysis of SVC's impact on bifurcation, chaos and voltage collapse in power systems. *Int J Electr Power Energy Syst* 2011;33:1194–202.
- [5] Hassan LH, Moghavvemi M, Almurib HAF, Steinmayer O. Current state of neural networks applications in power system monitoring and control. *Int J Electr Power Energy Syst* 2013;51:134–44.
- [6] Dillon TS, Niebur D. Neural networks applications in power systems. CRL Publishing Ltd; 1996.
- [7] Chakrabarti S, Jeyasuria B. On-line voltage stability monitoring using artificial neural network. In: Large engineering systems conference on power engineering, Halifax, Canada; 2004. p. 71–5.
- [8] El-Keib AA, Ma X. Application of artificial neural networks in voltage stability assessment. *IEEE Trans Power Syst* 1995;10(4):1890–6.
- [9] Chakrabarti S. Voltage stability monitoring by artificial neural network using a regression-based feature selection method. *Expert Syst Appl* 2008;35(4):1802–8.
- [10] Repo S. General framework for neural network based real-time voltage stability assessment of electric power system. In: IEEE midnight-sun workshop on soft computing methods in industrial applications, Finland; 1999.
- [11] Zhou DQ, Annakkage UD, Rajapakse AD. Online monitoring of voltage stability margin using an artificial neural network. *IEEE Trans Power Syst* 2010;25(3):1566–74.
- [12] Popovic D, Kukolj D, Kulic F. Monitoring and assessment of voltage stability margins using artificial neural networks with a reduced input set. *IEE Gener Transm Distrib* 1998;145(4):355–62.
- [13] Vakil-Baghmisheh MT, Razmi H. Dynamic voltage stability assessment of power transmission systems using neural networks. *Energy Convers Manage* 2008;49:1–7.
- [14] Kamalasadani S, Thukaram D, Srivastava AK. A new intelligent algorithm for online voltage stability assessment and monitoring. *Int J Electr Power Energy Syst* 2009;13:100–10.
- [15] Arya LD, Titare LS, Kothari DP. Determination of probabilistic risk of voltage collapse using radial basis function (RBF) network. *Electr Power Syst Res* 2006;76:426–34.
- [16] Jainn T, Srivastava L, Singh SN. Fast voltage contingency screening using radial basis function neural network. *IEEE Trans Power Syst* 2003;18(4):1359–66.
- [17] Chakrabarti S, Jeyasurya B. Multicontingency voltage stability monitoring of a power system using an adaptive radial basis function network. *Int J Electr Power Energy Syst* 2008;30:1–7.
- [18] Chakrabarti S, Jeyasurya B. An enhanced Radial Basis Function Network for voltage stability monitoring considering multiple contingencies. *Electr Power Syst Res* 2007;77:780–7.
- [19] Hashemi S, Aghamohammadi MR. Wavelet based feature extraction of voltage profile for online voltage stability assessment using RBF neural network. *Int J Electr Power Energy Syst* 2013;49:86–94.
- [20] Devaraj D, Preetha Roselyn J. On-line voltage stability assessment using radial basis function network model with reduced input features. *Int J Electr Power Energy Syst* 2011;33:1550–5.
- [21] Karami A. Power system transient stability margin estimation using neural networks. *Int J Electr Power Energy Syst* 2011;33(4):983–91.
- [22] Echavarren FM, Lobato E, Rouco L. Steady-state analysis of the effect of reactive generation limits in voltage stability. *Electr Power Syst Res* 2009;79:1292–9.
- [23] Milano F. An open source power system analysis toolbox. *IEEE Trans Power Syst* 2005;20:1199–206.
- [24] Van Cutsem T, Vournas C. Voltage stability of electric power systems. Boston: Springer; 1998.
- [25] Canizares C. Voltage stability assessment, procedures and guides. In: IEEE power eng soc. power system stability subcommittee special publication; 2001.

- [26] Sydel R. *Practical bifurcation and stability analysis: from equilibrium to chaos*. New York: Springer; 1994.
- [27] Ajarapu V. *Computational techniques in voltage stability assessment and control*. New York: Springer; 2006.
- [28] Canizares C, Alvarado FL. Point of collapse and continuation methods for large AC/DC systems. *IEEE Trans Power Syst* 1993;8(1):1–8.
- [29] Canizares C, De Souza AZ, Quintana VH. Improving continuation methods for tracing bifurcation diagrams in power systems. In: *Proc. bulk power system voltage phenomena III seminar, Davos, Switzerland*; 1994. p. 349–58.
- [30] Fauset L. *Fundamentals of neural networks*. New Jersey: Prentice-Hall; 1994.
- [31] Haykin S. *Neural networks: a comprehensive foundation*. New Jersey: Prentice-Hall; 1999.
- [32] Riedmiller M, Braum H. A direct adaptive method for faster back-propagation learning: the RPROP algorithm. *IEEE Int Conf Neural Networks* 1993:586–9.
- [33] Canizares C. On bifurcations, voltage collapse and load modeling. *IEEE Trans Power Syst* 1995;10(1):512–22.
- [34] Amjady N, Velayati MH. Evaluation of the maximum loadability point of power systems considering the effect of static load models. *Int J Energy Convers Manage* 2009:3202–10.
- [35] Zambroni de Souza AC, Alves Da Silva AP, Jardim JLA, Silva Neto CA, Torres GL, Ferreira C, et al. A new contingency analysis approach for voltage collapse assessment. *Int J Electr Power Energy Syst* 2003;25(10):781–5.
- [36] Jia ZH, Jeyasurya B. Contingency ranking for online voltage stability assessment. *IEEE Trans Power Syst* 2000;15(3):1093–6.
- [37] Guyon I. Practical feature selection from correlation to causality. In: *Mining massive data sets for security*. Amsterdam: IOS Press; 2008. p. 27–44.
- [38] May RJ, Dandy GC, Maier HR. Review of input variable selection methods for artificial neural networks. In: *Artificial neural networks- methodological advances and biomedical applications*. Croatia; 2011.
- [39] Stoppiglia H, Dreyfus G, Dubois R, Oussar Y. Ranking a random feature for variable and feature selection. *J Mach Learn Res* 2003:1399–414.
- [40] Pai MA. *Energy function analysis for power system stability*. Kluwer Academic; 1989.
- [41] Gibbard M, Vowles D. *Simplified 14-generator model of the SE Australian power system*. Australia: The University of Adelaide; 2010.
- [42] Razmi H, Shayanfar HA, Teshnehlab M. Steady state voltage stability with AVR voltage constraints. *Int J Electr Power Energy Syst* 2012:650–9.
- [43] Demuth H, Beale M, Hagan M. *neural networks toolbox user's guide for use with matlab 7*. The Mathworks Inc; 2006. Available at: <<http://www.mathworks.com/>>.
- [44] Hagan MT, Menhaj M. Training feedforward networks with the Marquardt algorithm. *IEEE Trans Neural Networks* 1994;5(6):989–93.